Occupied Bandwidth Comparison of BBOST-CPM with Two Transmit Antennas

Kazuyuki Morioka*, Naoki Kanada*, Shunichi Futatsumori*, Akiko Kohmura*,
Naruto Yonemoto*, Yasuto Sumiya* and David Asano†
*Electronic Navigation Research Institute 7-42-23, Jindaiji-higashi, Chofu, Tokyo, 182-0012, Japan.
†Faculty of Engineering, Shinshu University, 4-17-1, Wakasato, Nagano, 380-8553, Japan.
Email: morioka@enri.go.jp

***Abstract*—Continuous phase modulation (CPM) has constant envelope and good spectral properties, so it is suitable for satellite communication systems which require high power amplifiers. On the other hand, recent broadband mobile communication systems use space time block codes (STBC) to achieve channel gain by using multiple antennas. Burst based orthogonal space time-continuous phase modulation (BBOST-CPM) is a combination of orthogonal STBC and CPM which takes advantages of both merits. In this paper, we compare the occupied bandwidth of BBOST-CPM with two transmit antennas. We consider the relationship between modulation parameters and occupied bandwidth in detail. The results are useful for designing BBOST-CPM for future satellite communication systems.**

I. Introduction

Continuous phase modulation (CPM) [1][2] has a constant envelope property, so it can be used with a non-linear power amplifier. Also, CPM's spectral properties are good due to the phase continuity which keeps the side lobes low. Moreover, CPM can be thought of as a kind of coding modulation. The bit error rate can be improved by using multiple symbol detection at the receiver. As CPM has such good properties, it is suitable for satellite communication systems which requires high power amplifiers and high signal to noise ratios.

Recently, multiple-input and multiple-output (MIMO) has became an essential technique for broadband mobile communication systems. MIMO is divided into two categories: SM and STC. Spatial multiplexing (SM) increases channel capacity by transmitting data in parallel [3]. On the other hand, space time coding (STC) achieves diversity gain by sending the same data via multiple antennas and combining them at the receiver [4][5].

STC has big advantages for satellite communication systems which require high reliability and high sensitivity. While conventional STC is designed for linear modulation schemes such as phase shift keying (PSK) and quadrature amplitude modulation (QAM), we discuss STC for non-linear modulation schemes such as CPM.

STC is divided into space time trellis codes (STTC) [4] which use trellis codes and space time block codes (STBC) [5] which use orthogonal block codes. STTC with CPM is studied in [6]. However, the number of states in the trellis increases exponentially as the number of transmit antennas increases. This is the same problem as STTC with linear modulation schemes. Although this problem was solved by using STBC for linear modulation, direct adaptation of STBC for CPM breaks the continuity of phase and the orthogonality of STBC.

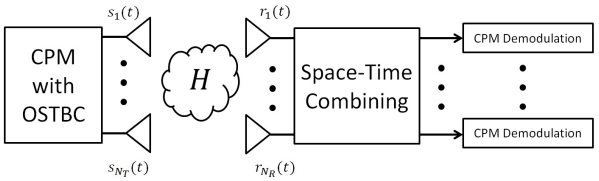

Fig. 1. System model for BBOST-CPM.

Wang and Xia solved this problem by introducing additional phase continuous function [7][8]. However, designing additional phase continuous functions to keep continuity and orthogonality becomes difficult as the number of transmit antennas increase. The maximum number of transmit antennas proposed so far is four [8].

On the other hand, Silvester, et.al. proposed burst based orthogonal space time coding [9]. In their scheme, CPM is adapted to STC block by block which enables the adaptation of CPM to conventional STBC naturally. We call their scheme burst based orthogonal space time-CPM (BBOST-CPM) as described in [10]. To the authors' knowledge, there have not been any studies that evaluate its occupied bandwidth. In this paper, we study the relationship between CPM parameters and the occupied bandwidth of BBOST-CPM.

The rest of this paper is organized as follows. In section 2, we review the system model of BBOST-CPM [9]. Then, we compare the occupied bandwidth with several CPM parameters in section 3. Finally, conclusions and future research are described in section 4.

II. System Model

We review the system model of BBOST-CPM according to [9]. Direct adaptation of CPM to STBC breaks the continuity of phase and orthogonality of STBC. Silvester, et.al. [9] proposed burst based orthogonal space time coding. Then, they adapted CPM to STBC naturally by inserting a guard time between blocks. Figure 1 shows the system model for BBOST-CPM which has N_T transmit antennas and N_R receive antennas. As shown in figure 1, it is possible to use a conventional CPM demodulation scheme after combining the coded data at the receiver.

The CPM modulated wave $x_{n_c}(t), 1 \leq n_c \leq N_C$ is described as follows.

$$x_{n_c}(t) = \sqrt{\frac{E_s}{T}} \exp\left(j2\pi h \sum_{i=0}^{N_B-1} a_{n_c}[i] q(t - iT) \right). \quad (1)$$

Here, $q(t)$ is a phase smoothing function defined as,

$$q(t) = \int_{-\infty}^{t} g(\tau) d\tau. \quad (2)$$

Here, $g(t)$ is a frequency pulse waveform defined over $0 \leq t \leq LT$, and is zero when $t < 0$ or $t > LT$. Moreover, h is the modulation index of CPM and the symbols $a_{n_c}[i] \in \mathcal{A}, 0 \leq i \leq N_B - 1$ are taken from the alphabet $\mathcal{A} = \{-M+1, -M+3, \ldots, M-3, M-1\}$ according to the transmitted symbols. Here, M is the modulation order. Also, E_s, T, N_B and N_C describe the energy per symbol, the symbol duration, the number of data symbols and the number of CPM waveforms, respectively. Here, the number of termination symbols N_E in [9] is set to zero for simplicity because it can be demodulated without termination.

For example, by using Alamouti's code [5]

$$\mathcal{O}_{2,2} \triangleq \begin{bmatrix} x_1 & x_2 \\ -x_2^* & x_1^* \end{bmatrix}, \quad (3)$$

the transmitted BBOST-CPM signal $s_{n_t}(t), n_t = \{1, 2\}$ becomes as follows [9].

$$s_1(t) = \begin{cases} \frac{1}{\sqrt{2}} x_1(t), & 0 \leq t \leq T_B, \\ -\frac{1}{\sqrt{2}} x_2^*(t - T_{tot}), & T_{tot} \leq t \leq T_{tot} + T_B, \end{cases} \quad (4)$$

$$s_2(t) = \begin{cases} \frac{1}{\sqrt{2}} x_2(t), & 0 \leq t \leq T_B, \\ \frac{1}{\sqrt{2}} x_1^*(t - T_{tot}), & T_{tot} \leq t \leq T_{tot} + T_B. \end{cases} \quad (5)$$

Here, we define $T_B \triangleq N_B T$, T_G is the guard time, and $T_{tot} \triangleq T_B + T_G$. The ratio of the guard time T_G to T_B is defined as R_G. Although we use Alamouti's code as an example, arbitrary STBCs can be used as noted in [9].

The received data $r_{n_r}(t)$ is described as follows.

$$r_{n_r}(t) = \sum_{n_t=1}^{N_T} h_{n_t n_r} s_{n_t}(t) + n_{n_r}(t), \quad 1 \leq n_r \leq N_R. \quad (6)$$

Here, the channel gains $h_{n_t n_r}$ are i.i.d. zero-mean Gaussian random variables with variance equal to one. $n_{n_r}(t)$ denotes an additive white Gaussian noise (AWGN) process with power spectral density N_0.

III. Bandwidth Comparison

Occupied bandwidth isn't considered in [9]. We study the relationship between CPM parameters and occupied bandwidth of BBOST-CPM in this section. We used computer simulations as analytical derivation of the occupied bandwidth of BBOST-CPM is very difficult.

Here, we change the phase to the next symbol point continuously in the guard time to preserve the phase continuity, while in [9] the transmitted power is gradually reduced to zero in the guard time to change to the next symbol point .

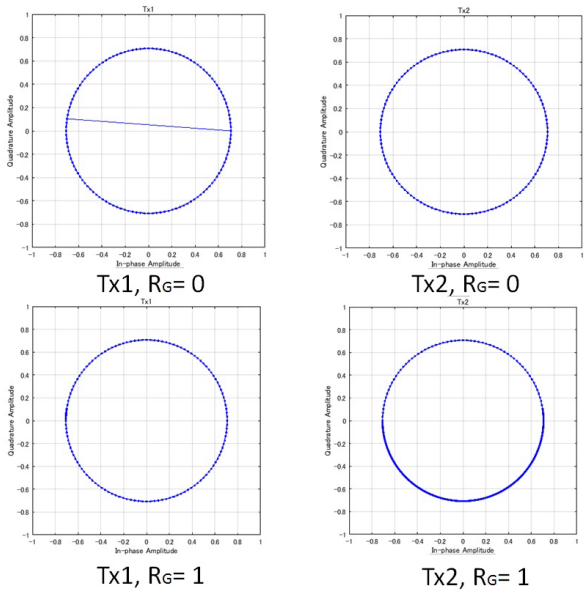

Fig. 2. Constellations of MSK for transmit antenna 1 and 2 when the guard time ratios are 0 and 1, respectively.

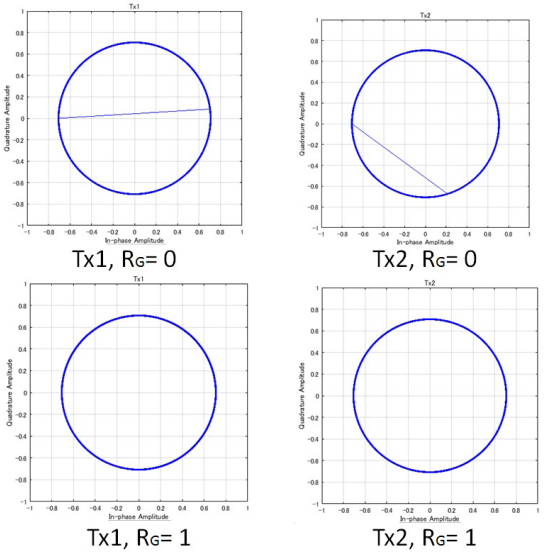

Fig. 3. Constellations of GMSK for transmit antenna 1 and 2 when the guard time ratios are 0 and 1, respectively.

We assume the number of transmit antennas N_T is two and the number of receive antennas N_R is one. Also, the modulation order M is 4, the block length N_B is 100. Figure 2 and 3 show the constellations of minimum shift keying (MSK) and Gaussian minimum shift keying (GMSK), respectively. These are typical CPM modulation formats. MSK is created when the pulse waveform $g(t)$ in (2) is a rectangular wave, the pulse length L is one, and the modulation index h is 0.5. GMSK is a special case of MSK when the pulse is a Gaussian pulse. Figure 2 and 3 show that there are discontinuous points if R_G is 0. Here, R_G represents the ratio of the guard time to the block length. On the other hand, phase discontinuity disappears when $R_G = 1$.

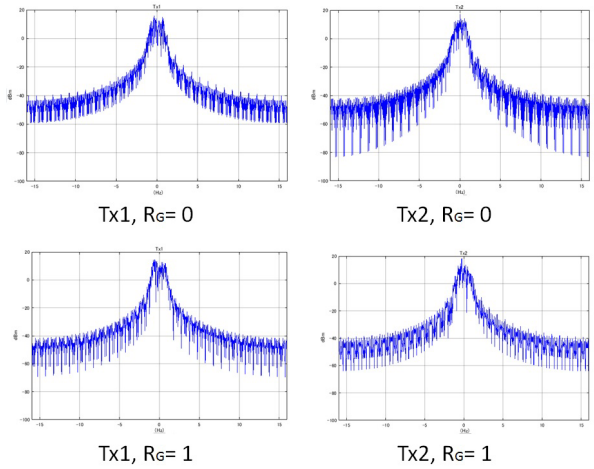

Fig. 4. Normalized power spectrum of MSK for transmit antenna 1 and 2 when the guard time ratios are 0 and 1, respectively.

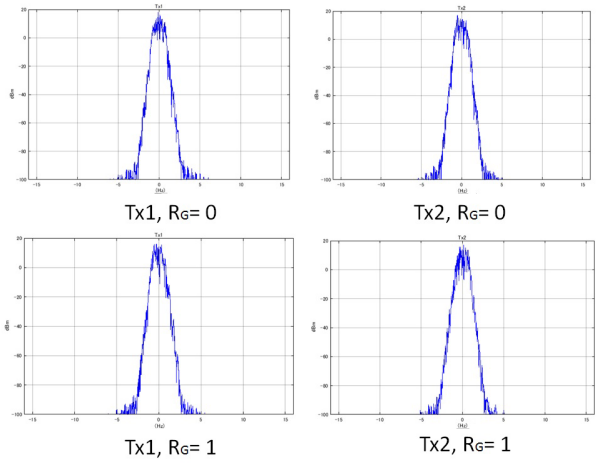

Fig. 5. Normalized power spectrum of GMSK for transmit antenna 1 and 2 when the guard time ratios are 0 and 1, respectively.

Figure 4 and 5 show the normalized power spectrum of MSK and GMSK, respectively. In this paper, we use the 99% bandwidth as the definition of bandwidth which is typically used in bandwidth evaluation. The 99% bandwidth is the bandwidth which contains 99% of the total power in figure 4 and 5. We calculate the bandwidth values by evaluating the mean value of 1000 trials. Also, we use the mean value of the 99% bandwidth of antenna 1 and antenna 2 as the system bandwidth. Hereafter, we use the system bandwidth to compare the occupied bandwidth.

Figure 6 describes how the occupied bandwidth decreases according to the length of the guard time. The horizontal axis is the guard time ratio (R_G). The vertical axis represents how the occupied bandwidth decreases. The unit is Hz and the amount of reduction increases as the value increases. In the figure, 1REC denotes the waveform when $g(t)$ in (2) is a rectangular wave and the pulse length L is one. 3RC denotes the waveform when $g(t)$ is a raised cosine wave and L is three. 3TFM denotes the waveform when $g(t)$ is a tamed frequency

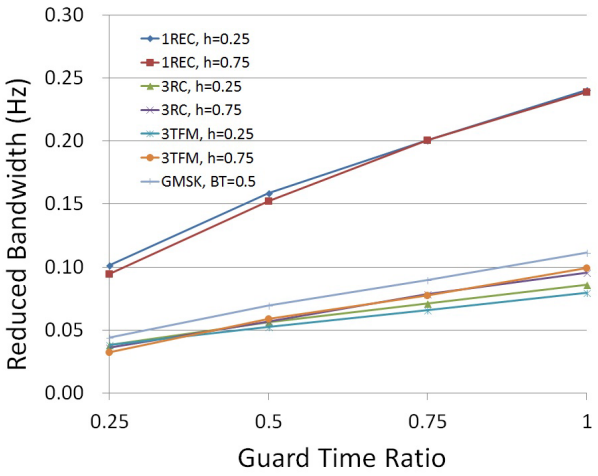

Fig. 6. Relationship between the guard time ratio and the reduced bandwidth for several CPM parameters.

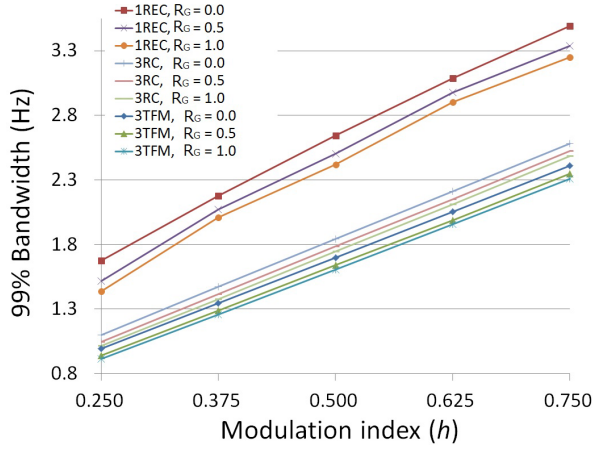

Fig. 7. Comparison of the 99% bandwidth for 1REC, 3RC and 3TFM when the guard time ratios are 0.0, 0.5 and 1.0, respectively.

modulation (TFM) pulse and L is three.

Figure 6 shows that the occupied bandwidth decreases when the guard time increases as the phase changes slowly. The occupied bandwidth decreases more than 0.1 Hz when the pulse wave is 1REC. Here, note that there is a tradeoff between the reduction effects and transmission rate. The transmission rate decreases when the guard time ratio increases.

Figure 7 shows the 99% bandwidth with several CPM parameters. The horizontal axis is the modulation index h and the vertical axis is the 99% bandwidth. We compared 1REC, 3RC and 3TFM when R_G is 0.0, 0.5 and 1.0. Figure 7 shows that the occupied bandwidth increases as the modulation index h increases, which is the same as in the single input and single output (SISO) case. Also, the occupied bandwidth decreases significantly when using 3RC or 3TFM. Figure 7 shows that the modulation index h and pulse waveforms affect the occupied bandwidth more than the guard time ratio.

Figure 8 shows the 99% bandwidth for GMSK. The horizontal axis is the 3dB bandwidth of the Gaussian pulse BT

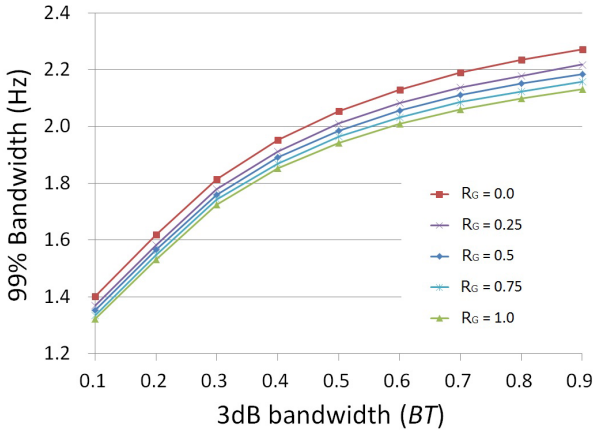

Fig. 8. Comparison of the 99% bandwidth for GMSK when the guard time ratios are 0.0, 0.25, 0.5, 0.75 and 1.0.

TABLE I. 99% BANDWIDTH FOR CPM.

Phase smoothing function (q)	Guard time ratio (R_G)	Modulation index (h)				
		0.25	0.375	0.5	0.625	0.75
1REC	0.0	1.6269	2.1267	2.5912	3.0382	3.4400
	0.25	1.5255	2.0623	2.5082	2.9697	3.3455
	0.5	1.4685	2.0233	2.4523	2.9287	3.2879
	0.75	1.4262	1.9844	2.4083	2.8905	3.2394
	1.0	1.3865	1.9587	2.3673	2.8543	3.2012
3RC	0.0	1.0514	1.4230	1.7917	2.1602	2.5324
	0.25	1.0129	1.3825	1.7535	2.1207	2.4963
	0.5	0.9953	1.3646	1.7337	2.1008	2.4758
	0.75	0.9805	1.3463	1.7160	2.0825	2.4541
	1.0	0.9654	1.3284	1.6969	2.0608	2.4367
3TFM	0.0	0.9446	1.2968	1.6462	2.0029	2.3588
	0.25	0.9064	1.2560	1.6120	1.9638	2.3262
	0.5	0.8923	1.2392	1.5913	1.9388	2.3000
	0.75	0.8788	1.2214	1.5710	1.9260	2.2813
	1.0	0.8650	1.2090	1.5566	1.9087	2.2598

and the vertical axis is the 99% bandwidth. We compared the occupied bandwidth when R_G is 0.0, 0.25, 0.5, 0.75 and 1.0. Figure 8 shows that the occupied bandwidth increases as BT increases which is the same as in the SISO case. Figure 8 shows that the 3dB bandwidth of the Gaussian pulse affects the occupied bandwidth more than the guard time ratio.

Finally, table I and II summarize the 99% bandwidths of CPM and GMSK. These results are useful for designing BBOST-CPM. Here, it is important to consider the transmission rate, bit error rate, complexity of demodulation and so on in order to design the system parameters. We are planning to study these tradeoffs in the future.

IV. CONCLUSION

In this paper, we compared the occupied bandwidth of BBOST-CPM which has advantages of both CPM and orthogonal STBC. We showed that the occupied bandwidth could be decreased by using a guard time. The reduction effect was more than 0.1 Hz when the pulse waveform and the pulse length were a rectangular wave and one, respectively. Also, we found that the occupied bandwidth decreased more significantly by changing the modulation parameters rather than the guard time length. We calculated the occupied bandwidth with several parameters for CPM. The results are useful for designing BBOST-CPM for future satellite communication

TABLE II. 99% BANDWIDTH FOR GMSK.

Guard time ratio (R_G)	3dB bandwidth (BT)		
	0.1	0.2	0.3
0.0	1.4017	1.6183	1.8146
0.25	1.3690	1.5827	1.7802
0.5	1.3522	1.5668	1.7601
0.75	1.3348	1.5475	1.7422
1.0	1.3225	1.5320	1.7250

Guard time ratio (R_G)	3dB bandwidth (BT)		
	0.4	0.5	0.6
0.0	1.9527	2.0543	2.1295
0.25	1.9125	2.0103	2.0831
0.5	1.8909	1.9847	2.0563
0.75	1.8698	1.9648	2.0316
1.0	1.8522	1.9429	2.0100

Guard time ratio (R_G)	3dB bandwidth (BT)		
	0.7	0.8	0.9
0.0	2.1894	2.2341	2.2723
0.25	2.1377	2.1783	2.2177
0.5	2.1100	2.1509	2.1850
0.75	2.0856	2.1240	2.1572
1.0	2.0607	2.0995	2.1321

systems. Finally, it is important to consider other performance measures such as transmission rate, bit error rate, complexity of demodulation and so on in order to design system parameters. We are planning to study the tradeoffs of these performance measures in the future.

ACKNOWLEDGMENT

Part of this work was supported by JSPS KAKENHI Grant Number 15K18073.

REFERENCES

[1] T. Aulin and C. Sundberg, "Continuous phase modulation–Part I: Full response signaling," Communications, IEEE Transactions on, vol.29, no.3, pp.196–209, 1981.

[2] T. Aulin, N. Rydbeck, and C. Sundberg, "Continuous phase modulation–Part II: partial response signaling," Communications, IEEE Transactions on, vol.29, no.3, pp.210–225, 1981.

[3] Foschini, G.J., "Layered space-time architecture for wireless communication in fading environment when using multi-element antennas, Bell Labs Technical Journal, vol.1, no.2, pp.41–59, 1996.

[4] V. Tarokh, N. Seshadri, and A. Calderbank, "Space-time codes for high data rate wireless communication: Performance criterion and code construction," IEEE Transactions on Information Theory, vol.44, no.2, pp.744–765, 1998.

[5] S.M. Alamouti, "A Simple Transmit Diversity Technique for Wireless Communications," IEEE Journal on Selected Areas in Communications, vol.16, no.8, pp.1451–1458, 1998.

[6] Xiaoxia Zhang and Fitz, M.P., "On the achievable rate/diversity for CPM MIMO fading channel," Proceedings. IEEE International Symposium on Information Theory 2003., pp.98, 2003.

[7] Genyuan Wang and Xiang-Gen Xia, "An orthogonal space-time coded CPM system with fast decoding for two transmit antennas," Information Theory, IEEE Transactions on, vol.50, no.3, pp.486–493, 2004.

[8] Genyuan Wang and Su, W. and Xia, Xiang-Gen, "Orthogonal-Like Space-Time-Coded CPM Systems With Fast Decoding for Three and Four Transmit Antennas," Information Theory, IEEE Transactions on, vol.56, no.3, pp.1135–1146, 2010.

[9] Silvester, A.-M., Schober, R. and Lampe, L., "Burst-Based Orthogonal ST Block Coding for CPM," Wireless Communications, IEEE Transactions on, vol.6, no.4, pp.1208–1212, 2007.

[10] Pande, Tarkesh and Heon, Huh and Krogmeier, James and David, Love., "Non-coherent Receivers for Orthogonal Space-Time CPM," Communications, IEICE Transactions on, vol.92, no.6, pp.2072–2084, 2009.